material exhibits changes which follow a bimodal pattern (Fig. 2), the higher values indicating a relatively high absorption by PAF-stained material around the nucleus, the lower values a relatively high absorption toward the axon. Again the variance in the position of a maximum or minimum between individuals, between strains, or between different staining techniques is up to 3 hours; the highest value, however, for the ratio of "circumnuclear" to peripheral absorption remains consistently at dawn. These bimodal changes in the distribution of neurosecretory material suggest a flow from the nucleus to the axon, the release of these granules into the neural pathway occurring at the middle or end of every light and dark phase. This can be confirmed by the observation that neurosecretory granules appear in the corpus cardiacum mainly 3 hours before dawn and dusk, whereas no granules can be detected shortly after the transition from light to dark.

The bimodal pattern of activity in neurosecretory cells, and in the corpus allatum has its parallel in the pattern of the locomotory activity (*6*) and oxygen consumption (*7*) which show peaks around dawn and dusk, so that neuro- and corpus allatum hormones may be a part of the activity controlling mechanism. The phase relation of corpus allatum cells to neurosecretory cells may suggest an activating influence from the corpus allatum hormone on neurosecretion as well as an inhibition in the opposite direction, which would amount to a negative feedback control (*8*). The transport of neurosecretory granules to the corpus cardiacum, the release, and the effect seem to occur within a few hours.

LUDGER RENSING
Biology Department, Princeton University, Princeton, New Jersey

References and Notes

1. H. Klug, *Wiss. Z. Humboldt-Univ. Berlin Math. Naturw. Reihe* **8**, 405 (1958-59); G. Mothes, *Zool. Jahrb. Abt. Allgem. Zool. Physiol. Tiere* **69**, 133 (1960).
2. M. Gabe, *Bull. Microscop. Appl.* **3**, 153 (1953).
3. G. Gomori, *Am. J. Pathol.* **17**, 395 (1941).
4. M. H. Flax and M. H. Himes, *Physiol. Zool.* **25**, 297 (1952).
5. H. Köpf, *Biol. Zentr.* **76**, 28 (1957).
6. L. A. Parry and L. P. Brower, unpublished senior thesis, Princeton University (1953).
7. L. Rensing, unpublished.
8. E. Scharrer and B. Scharrer, *Neuroendocrinology* (Columbia Univ. Press, New York, 1963).
9. I thank C. S. Pittendrigh for help and advice. This work was supported in part by funds from ONR [Contract Nonr 1858 (28) to C. S. Pittendrigh].

8 May 1964

Human Bone Marrow Distribution Shown in vivo by Iron-52 and the Positron Scintillation Camera

Abstract. *Radioactive iron, which concentrates in erythropoietic marrow, is given intravenously, and 16 hours later pictures of its distribution are taken with the positron camera. The instrument is an imaging device that produces pictures of the distribution of positron-emitting nuclides without scanning. Wide variations in the distribution of marrow are found in various diseases.*

The positron scintillation camera is a sensitive electronic instrument for producing pictures of the distribution of positron-emitting isotopes in vivo. Iron-52 is a cyclotron-produced positron-emitting isotope with a half-life of 8.2 hours. With this new instrument and isotope, we are taking relatively clear pictures of the distribution of erythropoietic marrow in living subjects; we use a dose of Fe^{52} that is within the limit permissible for diagnostic purposes. Less clear pictures of the distribution of marrow in the skeleton have been obtained in the past by the use of Fe^{59} and special scanning devices (*1*), but the positron camera and Fe^{52} provide information previously obtainable only by laborious postmortem examination.

Study of a number of cases has begun to yield characteristic patterns of bone marrow distribution for various disease states. In addition to being of potential diagnostic value, it is expected that these studies will aid our understanding of the pathogenesis of diseases of the bone marrow (*2*). This report deals with the technique and initial clinical results.

The positron scintillation camera has already been described (*3, 4*). It is being used to localize brain tumors with Ga^{68} EDTA (*5*), to study the deposition of F^{18} in bones and teeth of human subjects, and to determine the distribution of positron-emitting tracer compounds in small animals as a function of time after administration.

A diagram of the instrument is shown in Fig. 1. Immediately above the subject is an image detector consisting of a single sodium iodide crystal, 29 cm in diameter and 12 mm thick, activated by thallium—viewed by an array of multiplier phototubes. Below the subject is a focal detector consisting of an array of 19 scintillation counters with separate crystals. Both detectors remain stationary during the time a picture is being taken.

When a positron is emitted in tissue, it travels a few millimeters, and then combines with an electron. Two simultaneous annihilation gamma rays (0.51 Mev) are produced that travel away from the point of origin in opposite directions. The mean variation from 180 deg is 1/137 radian or ± 0.4 deg (*6*).

By use of a coincidence circuit and analog computing techniques, a two-dimensional readout of the distribution of the positron emitter is displayed as a series of position-oriented flashes of light on an oscilloscope. They are recorded on Polaroid film and an image of the distribution of the positron emitter results.

In the image detector, the phototubes are spaced about 7 cm from the crystal so that they view overlapping regions. When a scintillation occurs, the light divides among the tubes. The computing circuits sense the position of the scintillation and determine its x and y coordinates so that the scintillation can be displayed as a point of light on the oscilloscope if coincidence and pulse-height requirements are met. When scintillations occur at intermediate points between the phototubes, their position is still accurately determined because of the proportionate division of light among the tubes. The useful diameter of the crystal, over which an essentially undistorted image is obtained, is about 24 cm.

By summing the outputs from the phototubes, a signal is obtained that is proportional to the brightness of the scintillation without regard to where it occurred. This signal is sent to a pulse-height selector tuned to the photopeak of the 0.51-Mev gamma ray. Gamma rays that have lost an appreciable amount of energy by scattering are rejected. The same image detector is used with pinhole and multichannel collimators to display the distribution of nuclides that emit gamma rays (*4*).

For positron emitters, however, the focal detector and coincidence circuits are used because of the higher sensitivity achieved. Imagine a simplified version of the focal detector with only a single counter located at the center of the array shown in Fig. 1. When one gamma ray hits the counter, the other

impinges on the image detector. A coincidence circuit, which responds only to simultaneous pulses from the two detectors, allows the scintillation to be displayed on the oscilloscope. All scintillations that are not coincident with counts in the focal detector are not displayed. An image of the subject is effectively "projected" onto the image detector because the focal detector counter is a point of intersection for all gamma-ray pairs accepted by the coincidence circuit.

Each point in the subject is projected as a small disc on the image detector. The size of the disc is determined by the diameter of the focal detector crystal and the distances involved. To maintain good resolution, the focal detector crystal must be relatively small and far away from the subject, even though higher sensitivity could be obtained with a larger or closer crystal.

In practice 19 scintillation counters are used in the focal detector. With this arrangement high sensitivity is obtained, and at the same time good resolution can be maintained on any chosen plane within the subject. Compensating signals are sent from the focal detector array to the computer so that any point source on a chosen plane is imaged as a single disc on the oscilloscope, even though it is projected to a different place on the image detector by each of the 19 counters.

The correction is perfect for only one plane, since the computer can bring the 19 discs exactly together only for points lying on a single horizontal plane. This is called the "plane of best focus." Its location can be changed to any desired level in the subject by adjustment of the focal-plane selector—an attenuator in the electronic computing circuits. Although the parts of the subject lying on the plane of best focus are clearest, the compensation for other planes within 5 to 7 cm is almost exact, so they are shown in approximate focus (*7*). A certain "depth of focus" is obtained, just as with an optical camera.

The positron camera is sensitive to activity located on all planes within the subject. Those closest to the plane of best focus are most sharply resolved, but the camera responds with nearly equal sensitivity to activity on the other planes, and they are shown superimposed in the image.

The overall resolution is such that small sources of annihilation radiation no more than 9 mm apart in the subject can be resolved. At the same time, 1 μc of Fe^{52} in equilibrium with its radioactive daughter product results in about 2500 dots min^{-1} μc^{-1} on the picture, less the correction for tissue attenuation, which amounts to a factor of 2 for every 10 cm of soft tissue that the gamma rays penetrate. A more complete description of the positron scintillation camera is in preparation (*8*).

The Fe^{52} is produced by alpha bombardment of pure natural chromium in the Lawrence Radiation Laboratory 88-inch cyclotron. The principal reaction is

$$Cr^{50}\ (\alpha,\ 2n)\ Fe^{52}$$

The Fe^{52} is separated from the chromium by ether extraction (*9*), after the addition of 2 μg of carrier iron. The radioactive iron is then formed into a complex with citrate and made isotonic for intravenous injection. About 100 μc of Fe^{52} is obtained after chemical processing from a 1-hour bombardment.

Iron-52 has an 8.2 hour half-life

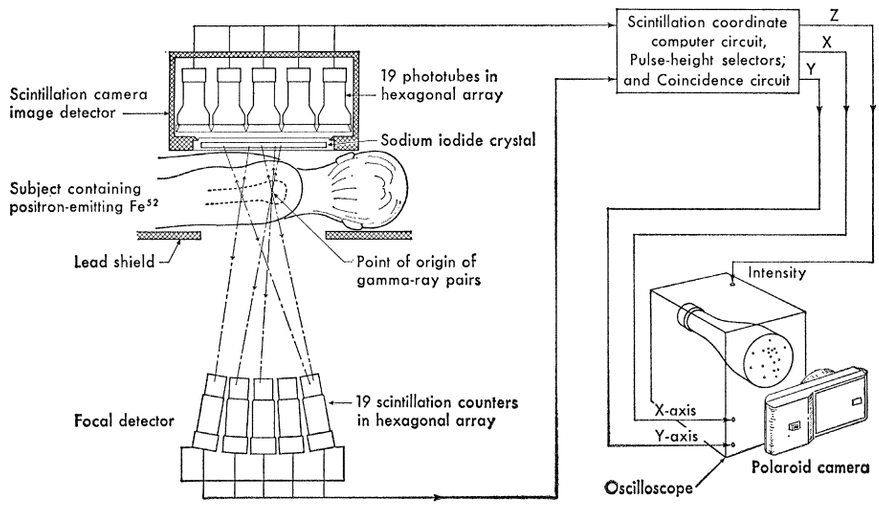

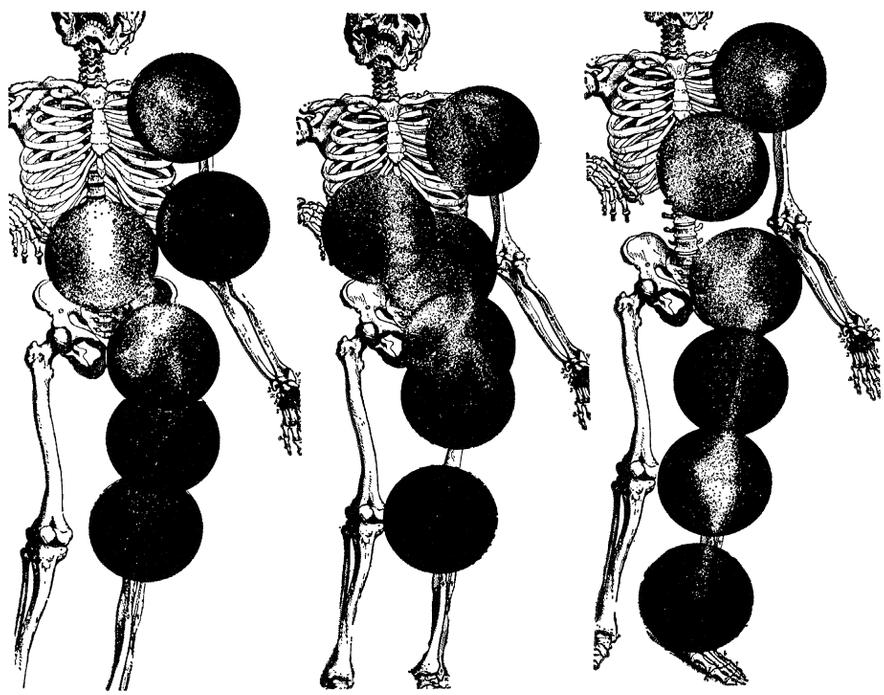

Fig. 1 (top). Block diagram of positron scintillation camera showing subject in position for picture of shoulder area. Bottom row: Fig. 2 (left). Bone marrow distribution in normal subject. Fig. 3 (middle). Bone marrow distribution in subject with mild cyanotic congenital heart disease. Fig. 4 (right). Bone marrow distribution in subject with polycythemia secondary to severe cyanotic heart disease.

and decays 57 percent by positron emission and 43 percent by electron capture to the radioactive daughter (metastable) Mn^{52m}. The daughter decays 100 percent by positron emission with a half-life of 21.3 minutes. The scintillation camera detects annihilation radiation from both nuclides, and there is no method of discriminating between them. This is a possible source of ambiguity in the pictures if the Mn^{52m} becomes free and able to travel about the body. However, there is no evidence that the Mn^{52m} does indeed become free. Manganese ion is removed from blood in the liver, but most patients examined by this method show no radioactivity in the liver. Those with known abnormal retention of iron in the liver have shown the expected uptake. The tentative conclusion has been made that the Mn^{52m} stays in the vicinity where it was formed by Fe^{52} decay, or at least does not concentrate in any specific organ.

The upper limit of radiation dose to the bone marrow of a normal adult has been calculated to be 2.5 roentgens for a 100-μc dose, if immediate uptake of the Fe^{52} in 1500 g of marrow is assumed, and if it is assumed that Mn^{52m} decays in the marrow. The irradiation is delivered almost entirely by positrons before they are converted to gamma-ray pairs. The average range of the positron is a few millimeters in soft tissue. Therefore the fat associated with marrow is irradiated, and its mass is included in the dose calculations.

A small amount of Fe^{55} ($\sim$ 5 μc) is produced when 100 μc of Fe^{52} is made by bombardment of natural chromium. The half-life of Fe^{55} is 2.6 years, but it decays entirely by electron capture and emits only 5.5-kev x-rays. This radiation is not detectable by the scintillation camera. The permitted continuous body burden of this isotope is 1 mc (*10*), so the few microcuries administered are of no practical consequence.

Pictures are taken about 16 hours after intravenous administration of 50 to 150 μc of Fe^{52}, when its uptake in marrow is maximum and its concentration in the blood is low. The field of view of the scintillation camera shows the marrow distribution in an area 20 cm in diameter with each exposure. Ten-minute exposures are taken of the areas where marrow may be found. To provide orientation, the pictures are cut out and glued to a drawing of a typical human skeleton. For this purpose, plate 21 of Vesalius's *Fabrica* is used. The size of the drawing is matched approximately to the patient's height.

This report is not intended to be a study of specific diseases, but rather it is a description of a new method and an illustration of the wide variations in marrow distribution that occur in association with different diseases. The cases have been chosen primarily to illustrate the remarkable differences in distribution of marrow within the body. The cases presented here may not be typical of their disease, and therefore the physiopathological significance of the observed changes in marrow distribution must await a more detailed study of each disease state.

Pictures of normal adult humans have shown a distribution pattern of erythropoietic marrow that agrees with the well-known clinical-pathological studies of the past. An example of the distribution in a 40-year-old male is shown in Fig. 2. It can be seen that marrow is located in the pelvis, spine, ribs, and the proximal ends of the extremities. In the legs, marrow is found in the area of the lesser trochanter of the femur and, in very small amounts, in the proximal one-fourth of the shaft. No significant amount is found in the area of the greater trochanter or in the head and neck of the femur. In the shoulder, marrow is shown in the glenoid fossa of the scapula and the distal end of the clavicle. It is also found in the proximal end of the humerus, with a small amount in the proximal one-half or one-quarter of the shaft. The spleen and liver do not accumulate sufficient iron to be seen under these conditions.

Two patients with polycythemia secondary to cyanotic congenital heart disease were studied. One was a 28-year-old man with mild cyanosis secondary to tetralogy of Fallot. He had a resting arterial oxygen saturation of 84 percent (normal 90 to 100 percent) and a total circulating red cell volume of 37 ml/kg (normal 24 to 33 ml/kg). The distribution of marrow in this patient, shown in Fig. 3, is comparable to that of the normal control except that the head and neck of the femur, which were not seen in the normal, are clearly seen.

The other patient with secondary polycythemia, a 46-year-old man with severe cyanosis secondary to tetralogy of Fallot, is shown in Fig. 4. This patient had a resting arterial oxygen saturation of 79 percent and a markedly elevated total circulating red cell volume of 69 ml/kg. His red cell production rate was 2.7 times normal, as determined by ferrokinetic studies. He was most unusual in that, in the plasma, the concentration of erythropoietin, the hormone that stimulates red cell production, was sufficiently elevated to be measurable in the starved-rat assay (*11*).

This patient had a very abnormal distribution of marrow. The entire femur, the proximal portion of the tibia, and the tarsal bones were observed. In the upper extremity, marrow extended distally to the middle of the forearm. There was a small amount in the bones of the wrist. In spite of the extensive peripheral extension of marrow, there was no evidence of extramedullary erythropoiesis in the spleen.

With the use of Fe^{52} and the newly developed positron scintillation camera, the bone marrow, a major organ of the body whose distribution could not be previously delineated in the living patient, can now be made visible with sufficient clarity to show the gross distribution. The first studies with this technique have demonstrated remarkable differences in marrow distribution associated with diseases of the blood-forming tissues. Marrow distribution studies may prove to be a valuable adjunct to diagnosis and may provide important additions to our knowledge of the physiopathological processes operating in a variety of disease states.

HAL O. ANGER
DONALD C. VAN DYKE
Donner Laboratory of Medical Physics and Biophysics, University of California, Berkeley 94720

References and Notes

1. H. O. Anger, *Am. J. Roentgenol. Radium Therapy Nucl. Med.* **70**, 605 (1953).
2. D. C. Van Dyke, H. O. Anger, M. Pollycove, *Blood*, in press.
3. H. O. Anger, in *Medical Radioisotope Scanning* (International Atomic Energy Agency, Vienna, 1959), pp. 59–73.
4. ———, *Nucleonics* **21**, No. 10 56 (1963).
5. ——— and A. Gottschalk, *J. Nucl. Med.* **4**, 326 (1963).
6. S. DeBenedetti, C. E. Cowan, W. R. Konecker, H. Primakoff, *Phys. Rev.* **77**, 205 (1950).
7. A. Gottschalk and H. O. Anger, in *Donner Laboratory Semiannual Report*, UCRL-11033 (1963).
8. H. O. Anger, "Positron scintillation camera," in preparation.
9. Extraction method by Y. Yano, modified from W. F. Hildebrand and G. F. Lundell, *Applied Inorganic Analysis* (Wiley, New York, 1953).
10. *Nat. Bur. Std. U.S. Handbook* **69** (1959), p. 30.
11. W. Fried, L. F. Plzak, L. O. Jacobson, E. Goldwasser, *Proc. Soc. Exptl. Biol. Med.* **94**, 237 (1957).
12. This work was supported by the U.S. Atomic Energy Commission. The use of Fe^{52} for this application was suggested by W. G. Myers of Ohio State University.

13 March 1964